



Research Paper

Heat pump-driven adsorption CO₂ capture for simple and cost-effective retrofits of coal power plantsSchalk Cloete^a, Antonio Giuffrida^b, Matteo C. Romano^b, Abdelghafour Zaabout^{a,c,*}^a Process Technology Department, SINTEF Industry, Trondheim, Norway^b Department of Energy, Politecnico di Milano, Milan, Italy^c ACER CoE Center, University Mohammed 6 Polytechnic, Ben Guerir 43150, Morocco

ARTICLE INFO

Keywords:

Adsorption CO₂ capture
Heat pump
Techno-economic assessment
Coal power plant
Decarbonization

ABSTRACT

Coal-fired power plants emit almost a third of fossil CO₂ emissions worldwide, and continued operation of existing plants will consume the entire remaining CO₂ budget for 1.5 °C of global warming. Hence, there is an urgent need to rapidly cut emissions from existing power plants. The continuous swing adsorption reactor (CSAR) concept offers a promising solution to this challenge. CSAR uses electrically powered heat and vacuum pumps to drive the CO₂ capture process and does not require the extraction of large amounts of steam from the power plant, greatly simplifying the retrofit process. A bottom-up techno-economic assessment of CSAR compared to conventional temperature swing adsorption (TSA) using the same sorbent showed near-identical performance in terms of energy penalty (8.0 for CSAR and 8.2 %-points for TSA) and CO₂ avoidance cost (54.1 €/ton for CSAR and 55.4 €/ton for TSA). Hence, retrofitting simplicity is achieved at no extra cost. The assessment also showed that, although new coal-fired power plants are economically unviable in regions with already high CO₂ prices, already depreciated plants will be difficult to displace via market forces. For example, the levelized cost of electricity for a coal power plant retrofitted with CSAR drops from 99.2 €/MWh to 68.2 €/MWh when the power plant is already depreciated. When CO₂ prices rise, the optimal strategy involves retrofitting plants located close to CO₂ storage or utilization opportunities for continued baseload operation, while unabated plants without easy access to storage are used at lower capacity factors to integrate rising shares of variable renewables. Simplified retrofitting via CSAR can facilitate the practical and economical execution of this strategy, achieving rapid decarbonization while minimizing the need for new capital investments and disruptive early asset retirements.

1. Introduction

The widely discussed 1.5 °C climate change mitigation scenario gives a CO₂ budget of 500 Gton CO₂ from the start of 2020 [1]. As of mid-2022, 100 Gton of this budget is already consumed, leaving 400 Gton. Existing and planned power plants will produce about 500 Gton of CO₂ over their lifetimes [2], mainly from coal. Thus, existing and soon-to-be-commissioned coal-fired power generation capacity will consume the entire remaining 1.5 °C CO₂ budget.

A big part of the reason for this disproportionate impact is that most operating coal plants are still very young. Out of the global fleet of just over 2000 GW of coal-fired generating capacity, 720 GW are younger than 10 years and an additional 630 GW is younger than 20 years [3]. Early forced retirement of most of this capacity and the associated

upstream supply industry will be very costly and disruptive, especially when considering that almost all of it is situated in developing nations where billions of people remain below decent living standards of 10–20 \$/day as illustrated by the global income distribution [4].

This is just one of the reasons why the recent special report on CO₂ capture and storage (CCS) as part of the International Energy Agency's Energy Technology Perspectives states that reaching net-zero without CCS will be virtually impossible [5]. In addition to the ability to decarbonize existing emitters (e.g., the large global fleet of relatively young coal-fired power plants) via retrofits, CCS also facilitates decarbonization of the most challenging emitters (heavy industry), the production of low-carbon fuels, and the removal of already emitted CO₂ from the atmosphere.

The present work is focused on the ability of CCS to decarbonize existing infrastructure, which will rely heavily on the development and

* Corresponding author at: Flow Technology Group, SINTEF Industry, S.P. Andersens vei 15 B, 7031 Trondheim, Norway.

E-mail address: abdelghafour.zaabout@sintef.no (A. Zaabout).

<https://doi.org/10.1016/j.applthermaleng.2023.121456>

Received 18 April 2023; Received in revised form 18 July 2023; Accepted 29 August 2023

Available online 30 August 2023

1359-4311/© 2023 The Authors. Published by Elsevier Ltd. This is an open access article under the CC BY license (<http://creativecommons.org/licenses/by/4.0/>).

Nomenclature			
Acronyms			
ACF	Annual cash flow	φ	Relative humidity (%)
APH	Air preheater	ϕ	Plant capacity factor (%)
BEC	Bare erected cost	a	Year in plant lifecycle (year)
CAC	CO ₂ avoidance cost	C	Annual cost (€/year)
CCS	CO ₂ capture and storage	C_p	Molar heat capacity (J/kmol.K)
CSAR	Continuous swing adsorption reactor	$C_{p,m}$	Mass heat capacity (J/kg.K)
CSTR	Continuous stirred tank reactor	E	Specific emissions (ton/MWh)
EPC	Engineering, procurement and construction	F	Molar flow rate (kmol/s)
FGD	Flue gas desulphurization	G	Mass flow rate (kg/s)
GGH	Gas-gas recuperative heater	h	Molar specific enthalpy (J/kmol)
LCOE	Levelized cost of electricity	h_m	Mass specific enthalpy (J/kg)
LP	Low pressure	i	Discount rate (%)
NPV	Net present value	M	Mass (kg)
OC	Owner's cost	N	Moles (kmol)
PC	Pulverized coal	P_{El}	Electricity sales price (€/MWh)
PEI	Polyethyleneimine	p	Partial pressure (kPa)
PS	Process contingency	Q	Heat flow (W)
PT	Project contingency	q	Sorbent loading (mol/kg)
SARC	Swing adsorption reactor cluster	R	Reaction rate (kmol/s)
SCR	Selective catalytic reduction	R_0	Universal gas constant (J/kmol.K)
SEA	Standardized economic assessment	S	Stoichiometric coefficient (-)
TOC	Total overnight cost	S_{El}	Annual electricity sales (MWh/year)
TSA	Temperature swing adsorption	T	Temperature (K)
USC	Ultra-supercritical	t	Time (s)
VPSA	Vacuum/pressure swing adsorption	U	Heat transfer coefficient (W/m ² K)
		V	Volume (m ³)
		x	Mass fraction (-)
		y	Mol fraction (-)
Symbols			
ΔH	Adsorption enthalpy (kJ/mol)		

deployment of practical and cost-effective post-combustion CO₂ capture technologies. At present, cost is a major barrier to CCS deployment, but large cost reductions are possible. For example, SaskPower, the operator of one of the two large-scale CCS operations from coal-fired power production that have been built and operated to date, estimates that costs can fall by 67% for a second generation CO₂ capture facility [6]. Once capture technologies reach sufficient scale and standardization, even first generation monoethanolamine (MEA) systems can achieve CO₂ avoidance costs of 44–86 \$/ton (excluding transport and storage) from coal-fired power production [7], which is well below projected medium-term CO₂ prices in many world regions. For example, the IEA Announced Pledges Scenario [8] assumes that CO₂ prices reach 135 \$/ton by 2030 in advanced economies and 110 \$/ton by 2040 in developing economies with net-zero pledges.

Significant further cost reductions could be achieved by commercializing second-generation capture technologies using advanced solvents [9], sorbents [10], or process integrations [11]. The rapid development of such second-generation CO₂ capture technologies is vital to avoid the lock-in of costlier first-generation technologies. For example, the key CCS deployment period envisioned for China is 2035–2045 [12]. If second generation technology is not made available in time, the economically viable CCS potential in China is only 0–144 GW [13], but this number increases to 144–431 GW if second-generation technology is ready for deployment by 2035. If the timeline is accelerated to 2030, the potential increases further to 431–500 GW.

Post-combustion CO₂ capture from power plants generally employs low-pressure steam extracted from the Rankine cycle to regenerate the solvent or sorbent [14], causing the primary energy penalty of CCS. There are different ways to do this integration. For example, the two large-scale coal power CCS projects that have been operated to date utilize very different philosophies with different advantages and

drawbacks [15]. The Boundary Dam plant uses steam directly from the coal plant, whereas the Petra Nova facility utilizes a separate gas-fired cogeneration plant to supply the regeneration heat and additional power. The study [15] found that the Petra Nova configuration offers significant cost and performance benefits, but it causes significant additional emissions from the unabated combustion of natural gas.

The Boundary Dam approach is the more generically applicable option for deep decarbonization, especially in Asia where 77% of the world's coal is consumed and most natural gas must be imported at high costs. In preparation for this CCS retrofitting rollout, the design of CCS-ready plants is important, although this also faces uncertainty about the steam conditions required by future CO₂ capture processes [16]. However, various configurations are possible to retrofit plants that were not built with CCS in mind with only minor efficiency penalties [16], although significant modifications to the power cycle are needed.

This paper investigates a different retrofitting philosophy using a CO₂ capture concept that utilizes only electrical energy as input, thus limiting or even avoiding any integration with the steam cycle that would increase the complexity of the retrofit project. The concept is derived from the swing adsorption reactor cluster (SARC) [17] that uses heat and vacuum pumps to regenerate the sorbent using a combination of temperature and vacuum swings. Competitive efficiencies are achievable in coal-fired power production [18], although the concept is most attractive for processes that do not have readily available low-grade heat for sorbent regeneration such as cement production [19,20]. However, given the increasing relevance of a rapid CCS retrofitting “gigaproject” of the world's large fleet of coal-fired power plants, this paper will compare the performance of the heat and vacuum pumps to the conventional use of low-pressure steam in this setting.

The concept is simulated in a sorbent looping configuration where a sorbent powder is circulated between an adsorber (where CO₂ is

captured) and a desorber (where it is released for compression and storage). When using combined heat and vacuum pumps, the concept is labelled as the continuous swing adsorption reactor (CSAR), whereas it is labelled temperature swing adsorption (TSA) when regeneration is carried out with steam from the power cycle. More details follow in the next section.

These two configurations were selected to facilitate a direct comparison between a CO₂ capture configuration that does not need integration with the host process and a more traditional post-combustion CO₂ configuration that requires large amounts of steam to be extracted from the steam cycle. The similarity in the process layouts of the two configurations will clearly isolate any penalty involved in replacing steam extraction with a heat and vacuum pump to simplify retrofit operations. More traditional (and experimentally demonstrated [21]) fixed bed sorbent-based vacuum/pressure swing adsorption (VPSA) could also have been considered as an electrically powered CO₂ capture process that facilitates easy retrofits. However, such configurations are not attractive for relatively dilute flue gases resulting from coal-fired power production (due to excessive reactor volumes and footprints), being better suited to pre-combustion configurations where the CO₂ partial pressure is much higher [22].

Novel contributions of the present study can be summarized as follows: 1) the first assessment of the techno-economic performance of the CSAR concept for retrofitting coal-fired power plants, 2) direct quantification of the cost of replacing steam extraction from the power plant with electrically powered heat and vacuum pumps for ease of retrofitting, and 3) new perspectives regarding the importance of practical and economical retrofits for the world's large fleet of coal-fired power plants in an environment of rising CO₂ prices.

The CSAR and TSA concepts are outlined in more detail in the next section, after which the general methodology employed in the techno-economic assessment is presented. Next, results detailing the benchmarking of CSAR against TSA and the effect of CCS retrofits and plant capacity factor on the competitiveness of coal-fired power plants in future electricity systems are presented and discussed. Finally, the study draws several novel conclusions regarding the optimal roles of CSAR and coal-fired power production going forward.

2. Description of the CSAR and TSA technologies

The operation of the CSAR concept is illustrated in Fig. 1 with stream data in Table 1. Sorbent is contacted with the flue gas in a counter-current manner in the adsorber where the heat pump removes heat to limit the temperature rise from the exothermic reactions. Perforated trays may be used in conjunction with purposefully designed heat transfer surfaces to restrict the axial mixing in the fluidized bed adsorber to facilitate counter-current behaviour, as has been demonstrated experimentally for the SARC concept [17]. Such counter-current operation ensures high CO₂ capture ratios by contacting the CO₂-lean flue gas with highly regenerated sorbent at the top of the column. An ammonia drum is assumed, allowing a pure liquid feed to the evaporator to ensure adequate working fluid distribution across the heat transfer surfaces.

The carbonated sorbent then flows into the bottom lock hopper, which is closed to allow for some of the N₂-rich gases to be evacuated to preserve high CO₂ purity. This small extracted flow contains some CO₂ and it is therefore fed back to the flue gas before the adsorber. After evacuation, the lock hopper is opened to the side of the desorber, allowing the sorbent to exit into the vacuum environment. The reduction in pressure causes some CO₂ and H₂O release to drive the sorbent up the riser tube into the desorber. In addition, some vacuum pressure steam or recirculated CO₂ can be fed to this line to ensure successful upwards transport of the sorbent. Moreover, injecting vacuum pressure steam raised from waste heat is an effective way to introduce an additional partial pressure swing and reduce costs without requiring difficult integration with the power plant.

Once inside the desorber, the sorbent is heated by the heat pump to facilitate additional CO₂ and H₂O release (combined temperature and vacuum swing). The resulting mixture of CO₂ and H₂O is extracted by the main vacuum pump at the top of the desorber.

Regenerated sorbent at the top of the desorber then flows into the top lock hopper. Once filled, the lock hopper is closed and a valve to the atmosphere is opened to pressurize the system. Upon reaching atmospheric pressure, the lock hopper is opened to the adsorber side so that the sorbent can fall into the cooler. After this step, the lock hopper is closed again and an evacuation pump extracts the air to reach the regeneration pressure and facilitate the entrance of the next batch of regenerated sorbent. Like the bottom lock hopper, this evacuated gas is also fed back into the flue gas to avoid CO₂ venting.

In the cooler, the heat pump extracts heat from the hot sorbent to reduce the equilibrium CO₂ partial pressure before entering the top of the adsorber to facilitate high CO₂ capture ratios. This unit is fluidized by a small stream of air to ensure good heat transfer. Similar to the evacuated streams from the lock hoppers, this stream is mixed with the flue gas.

Finally, some cooling water extracts additional heat at the top of the adsorber to minimize the equilibrium CO₂ partial pressure in this region, increasing the capture ratio. For simplicity, the cooling water was simulated to extract heat at a constant temperature of 25 °C from which the heat transfer rate was calculated according to Equation 9 listed in the following section. This assumption describes a heat exchanger where the inlet and outlet water temperatures are specified below and above the 25 °C average so as to achieve the simulated amount of heat transfer with the specified heat transfer surface area. From an overall energy balance perspective, additional heat extraction is needed to cancel out the heat generation by the heat pump and the heat introduced by the flue gas, which enters at a higher temperature than it exits the adsorber.

The frequency of the lock hopper fill-empty cycle allows precise control over the sorbent circulation rate. Since the lock hoppers have a fixed volume, the sorbent circulation rate is the product of the sorbent mass loading of the lock hopper and the frequency at which this mass is transferred from one reactor to the next. Fine-tuning of the sorbent distribution between the adsorber and desorber will also be possible via independent control of the top and bottom lock hoppers.

The TSA benchmark system is illustrated in Fig. 2 with stream data in Table 2. The adsorber, cooler, and desorber operate in a similar manner to the CSAR concept. However, in this case, cooling water extracts heat from the adsorber and the cooler at an average temperature of 25 °C (under the same assumptions as the water cooler at the top of the CSAR adsorber), whereas steam supplies heat to the desorber at a temperature required to achieve the desired CO₂ capture ratio. In addition, the desorber is much narrower to facilitate the lean conditions required to minimize pressure drop and ensure a sufficiently low pressure at the bottom to allow the sorbent to flow into the desorber. It is assumed that the desorbed gases can fluidize the bed, which, in practice, would require a conical vessel that is narrower at the bottom than the top. A small recycle from the CO₂-rich outlet stream may be required to ensure reliable operation, but it will have a minimal impact on the economic assessment.

Furthermore, the lock hoppers in the CSAR concept are replaced by heat exchangers that serve to recuperate heat from the hot regenerated sorbent for pre-heating the cold carbonated sorbent. Heat exchange is facilitated by a working fluid that circulates between the top and bottom heat exchangers in Fig. 2 to transport heat from the hot to the cold sorbent. The small air and flue gas streams used to fluidize these heat exchangers and the cooler contain some CO₂ and are therefore fed back to the flue gas upstream of the adsorber to avoid unnecessary CO₂ venting.

The higher desorber temperature required in the TSA process will accelerate sorbent deactivation relative to the CSAR process. Oxygen in the air used to fluidize the recuperative heat exchangers can accelerate the deactivation process (a 21% O₂ atmosphere approximately doubles

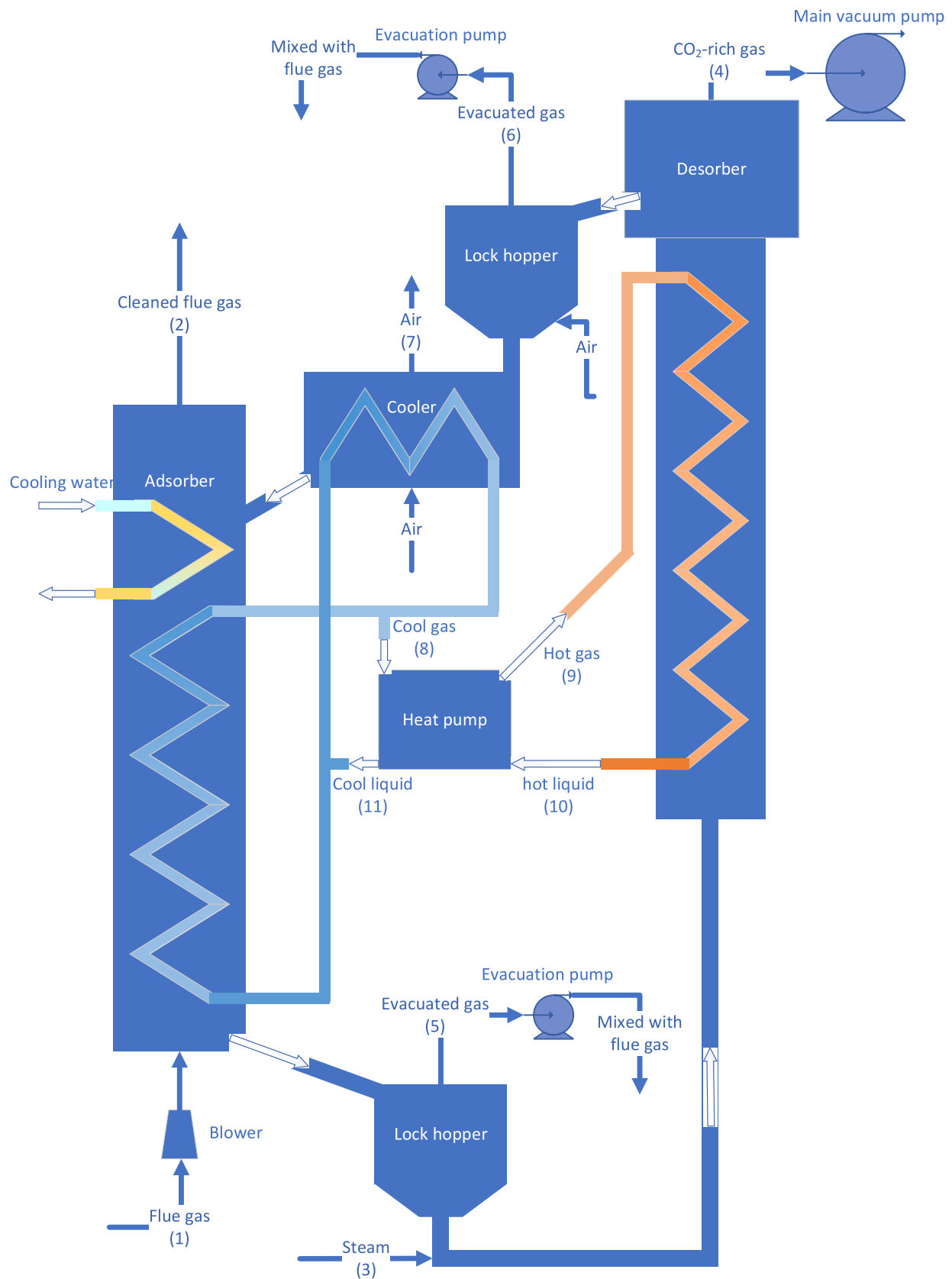


Fig. 1. Illustration of the CSAR concept.

Table 1

Stream table for the CSAR concept achieving a 90% CO₂ capture ratio according to the numbering in Fig. 1. Quality refers to the vapour fraction of saturated steam in stream 3 and saturated ammonia in streams 8–11.

No.	T (°C)	P (bar)	\dot{m} (kg/s)	Composition (mol%)					Quality (%)
				CO ₂	H ₂ O	N ₂	O ₂	NH ₃	
1	49.4	1.00	81.6	13.5	11.6	71.1	3.8		
2	54.3	1.00	61.7	1.6	3.9	89.7	4.8		
3	70.2	0.31	2.1		100.0				100.0
4	69.6	0.15	20.9	48.5	51.0	0.4	0.1		
5	70.4	0.70	0.9	27.9	15.3	53.9	2.9		
6	69.3	0.15	1.0	7.1	7.6	67.4	17.9		
7	55.9	1.00	0.8	1.9	4.2	74.2	19.7		
8	51.4	21.07	32.5					100.0	100.0
9	101.8	38.08	32.5					100.0	Super-heated
10	76.2	38.08	32.5					100.0	0.0
11	51.4	21.07	32.5					100.0	12.6

the deactivation rate relative to a case isolating thermal deactivation in an O₂-free atmosphere [23]). However, the sorbent will be rapidly cooled in the heat exchanger, limiting the time it is exposed to a combination of high temperatures and O₂ concentrations. Furthermore, the sorbent used in the current modelling uses epoxide functionalization to greatly reduce the impact of oxidative degradation [24].

Finally, the TSA concept will require a simple valve mechanism adjusting the resistance to particle flow between the reactors to achieve a similar level of control over the sorbent circulation rate as offered by the lock hoppers in the CSAR concept.

3. Methodology

The methodology is presented in three parts: reactor modelling, process modelling, and economic assessment.

3.1. Reactor modelling

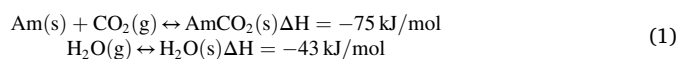
Both the CSAR and TSA reactor systems were modelled under the following simplifying assumptions:

- The reactor can be considered as a series of Continuous Stirred Tank Reactors (CSTR), which is a reasonable assumption when considering well-mixed fluidized beds.
- Sorbent powder and gas occupy each CSTR, and the gas is represented as a mixture of ideal gases – a valid assumption in this low-pressure system.
- There is thermal and chemical equilibrium between gas and solid. Fluidized beds feature very fast gas-particle heat transfer, ensuring thermal equilibrium. Reaction rates are also relatively fast for the chosen sorbent [17], closely approximating chemical equilibrium.

Based on these assumptions, which have been experimentally validated for the SARC process [25], the equation system described below was implemented in Matlab and solved using the ode15s solver.

3.1.1. Chemistry

Two equilibrium reactions are simulated for the polyethyleneimine (PEI) sorbent employed [26]: chemical adsorption of CO₂ on the amine (Am) group of the sorbent and physical adsorption of H₂O.



The Toth isotherm was used to describe the equilibrium sorbent loading of CO₂ (q_{CO_2}) [mol/kg] [26]:

$$q_{\text{CO}_2} = \frac{n_s b p_{\text{CO}_2}}{(1 - (b p_{\text{CO}_2})^t)^{\frac{1}{t}}} \quad (2)$$

$$n_s = n_{s,0} \exp\left(X\left(1 - \frac{T}{T_0}\right)\right) \quad (3)$$

$$b = b_0 \exp\left(\frac{dH}{RT_0} \left(\frac{T_0}{T} - 1\right)\right) \quad (4)$$

$$t = t_0 + \alpha \left(1 - \frac{T_0}{T}\right) \quad (5)$$

A linear fit with the relative humidity (ϕ) was used for the H₂O isotherm [26]. The model coefficients to use in Eq 1 to Eq 5 are specified in Table 3.

$$q_{\text{H}_2\text{O}} = \begin{cases} 5.69\phi + 0.2528 \\ 37.66\phi \text{ if } \phi < 0.0087 \end{cases} \quad (6)$$

3.1.2. Mass and energy balances

Mass balances are solved for the gas and the solids in each CSTR:

$$\begin{aligned} \frac{dN}{dt} &= F^{\text{in}} y^{\text{in}} - F y + S_g^T R \\ \frac{dM}{dt} &= G^{\text{in}} x^{\text{in}} - G x + S_s^T R \end{aligned} \quad (7)$$

Here, N [kmol] is a vector of the gas holdup of each species in the gas phase; F^{in} and F [kmol/s] are the molar flow rates of gas into and out of the CSTR; G^{in} and G [kg/s] are the mass flow rates of the solids into and out of the CSTR; $y = N/\text{sum}(N)$ [-] is a vector of gas mole fractions; $x = M/\text{sum}(M)$ [-] is a vector of solids mass fractions; M [kg] is a vector of the mass holdup for each solid species in the CSTR; S is the reaction stoichiometry matrix; and R is a vector of chemical reaction rates, assumed to be fast for rapidly approaching chemical equilibrium.

Following the assumption of thermal equilibrium, only one energy balance is solved, combining the effects of the gas and the solids phases:

$$(M^T C_{p,m,s} + N^T C_{p,g}) \frac{dT}{dt} = F^{\text{in}} (h_g^{\text{in}} - h_g) + G^{\text{in}} (h_{m,s}^{\text{in}} - h_{m,s}) - R^T \Delta H + Q \quad (8)$$

Here, $C_{p,m,s}$ [J/kg.K] and $C_{p,g}$ [J/kmol.K] are vectors of heat capacities of solids and gas species; T [K] is the reactor temperature; h_g^{in} and h [J/kmol] are the inlet and outlet gas enthalpies; $h_{m,s}^{\text{in}}$ and $h_{m,s}$ [J/kg] are the inlet and outlet solids enthalpies; ΔH [J/kmol] is a vector of the reaction enthalpies; and Q [W] is heat added or removed via the heat transfer surfaces, modelled as follows:

$$Q = UA\Delta T \quad (9)$$

Here, A [m²] is the heat transfer surface area in the CSTR, $U = 400$ W/m²K is the heat transfer coefficient measured from experiments [17], and ΔT [K] is the temperature difference between the reactor and the heat transfer fluid. A constant working fluid temperature is set in each

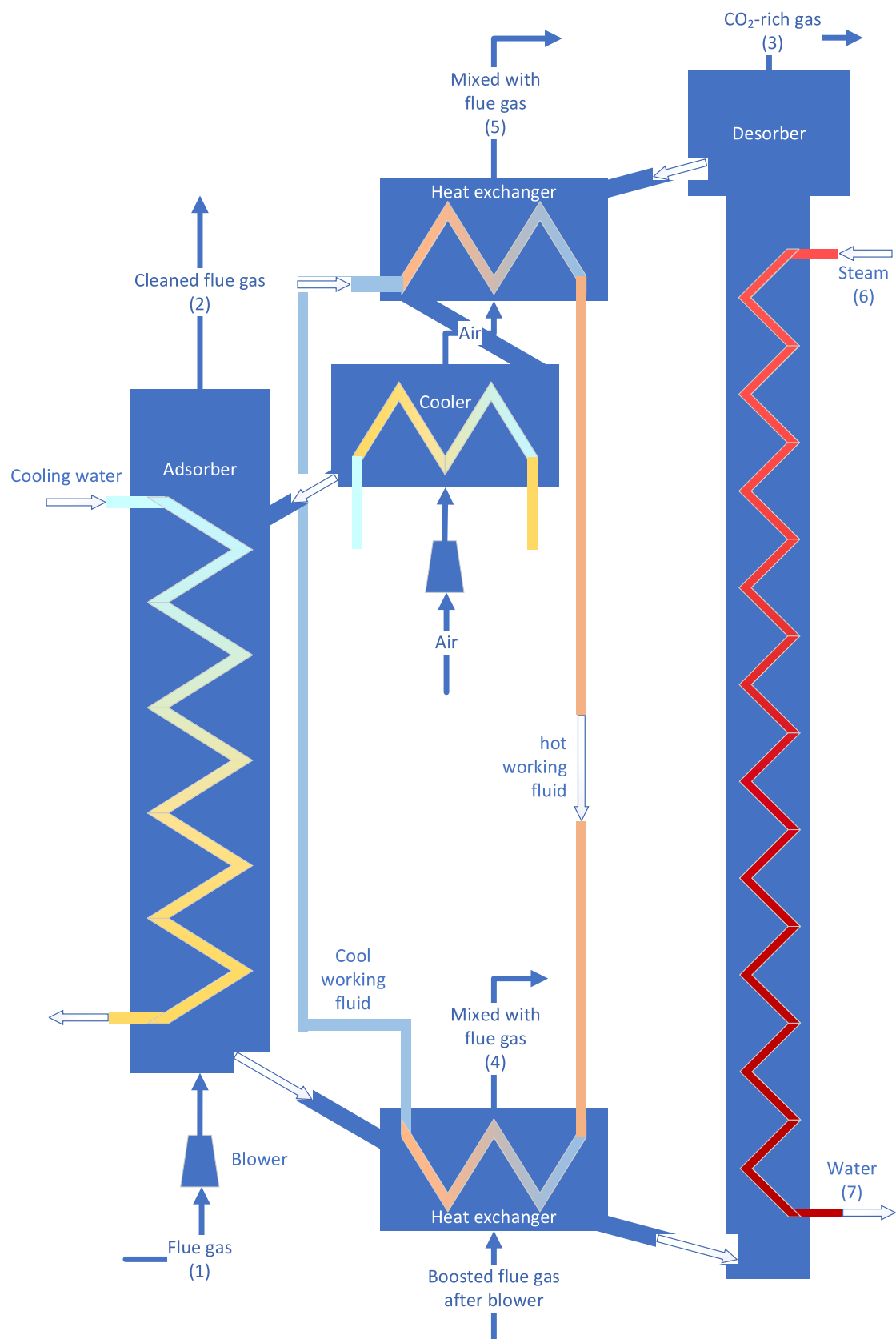


Fig. 2. Illustration of the TSA concept.

Table 2

Stream table for the TSA concept achieving a 90% CO₂ capture ratio according to the numbering in Fig. 2. Quality refers to the vapour fraction of saturated steam.

No.	T (°C)	P (bar)	\dot{m} (kg/s)	Composition (mol%)				Quality (%)
				CO ₂	H ₂ O	N ₂	O ₂	
1	49.6	1.00	81.2	13.8	11.7	70.9	3.7	
2	47.1	1.00	62.3	1.6	6.0	87.7	4.6	
3	87.8	1.00	17.9	64.3	35.2	0.5	0.0	
4	57.9	1.00	0.7	37.1	9.1	51.2	2.6	
5	78.6	1.00	1.3	28.5	25.1	36.7	9.7	
6	92.7	0.78	22.6		100.0			100.0
7	92.0	0.78	22.6		100.0			0.0

Table 3

Model coefficients for use in Equation 2 to Equation 5.

$n_{s,0}$	X	b_0	dH	t_0	α	T_0
2.146 mol/kg	0.317 –	38.25 1/kPa	104,581 J/mol	0.497 –	1.273 –	303 K

reactor due to the phase change operation of the heat pump working fluid. The constant temperatures in the two reactors are subsequently used in the process model to calculate the power consumption of the heat pump for CSAR and the temperature of steam extraction for TSA. Aside from the working fluid temperatures, all necessary stream details are also transferred to the process model.

As stated earlier, the assumption of a constant working fluid temperature is also used for cooling water under the simplifying assumption that the average cooling water temperature employed represents the water inlet and outlet temperatures that would result in the overall heat transfer rate calculated in Equation 9. Given that the reactor temperature is always more than 25 °C above the average cooling water temperature and the difference between cooling water inlet and outlet temperature is only 10 °C, this simplification will only have a minor effect on the distribution of heat transfer along the reactor height.

Finally, the ideal gas equation of state is used for the gas phase, as follows:

$$pV_g = \sum(N)R_0T \quad (10)$$

Here, p [Pa] is the pressure; V_g [m³] is the gas volume; and R_0 [J/kmol.K] is the universal gas constant.

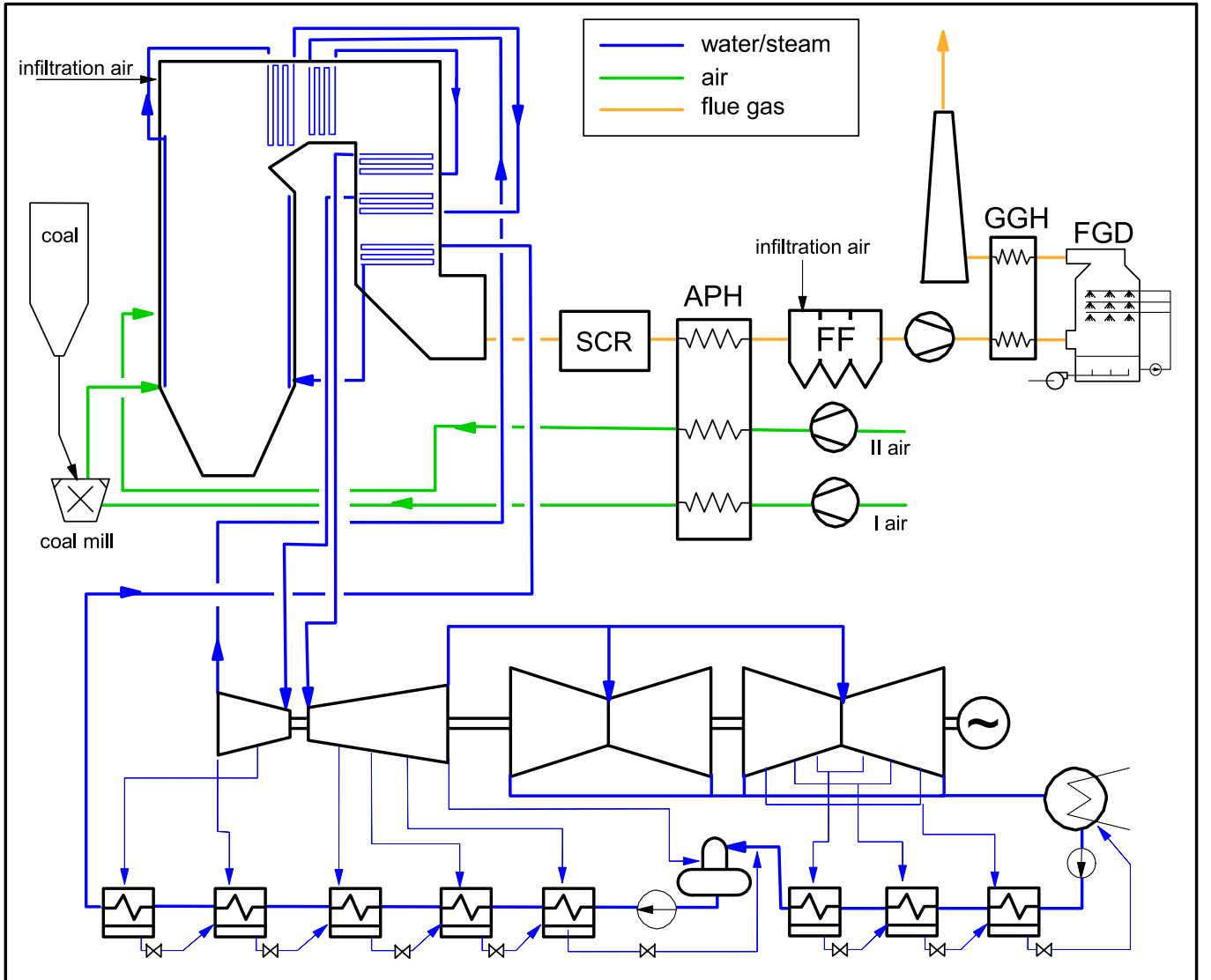


Fig. 3. Schematic of the reference power plant without CO₂ capture.

3.2. Power plant modelling

Both the CSAR and TSA processes described in [section 2](#) have been integrated into a large-scale power plant with an ultra-supercritical (USC) pulverized coal (PC) boiler generating superheated and reheated steam at 270/60 bar and 600/620 °C by burning 1657 MW_{LHV} of low sulphur bituminous coal for around 740 MW of net electric output [\[27\]](#).

The mass and energy balances of the power plants without and with CO₂ capture are calculated with the in-house code “GS”, which has been used by the authors in multiple previous works (e.g., the aforementioned modelling studies of the SARC concept applied to cement production [\[20\]](#) and coal power plants [\[18\]](#)). The main assumptions used for the calculations of the power plant are defined according to the European Benchmark Task Force guidelines [\[28\]](#) and are reported in the Appendix.

Details of the power plant as well as of the CO₂ capture system are reported in the next sections.

3.2.1. Power plant without CO₂ capture

The reference power plant without CO₂ capture is schematically shown in [Fig. 3](#). Primary and secondary air streams are heated up in a tri-sector Ljungström air preheater (APH). Primary air (25% of the total combustion air) is used for coal drying and for the transport of the pulverized coal from the mills to the burners. Secondary air is injected at different positions into the boiler according to an air-staging system for primary control of NO_x emissions. An O₂ content of 2.9% in the flue gas is maintained by a proper air excess. Heat losses have been also considered for incomplete combustion and radiation losses. Exhaust gases leave the boiler after the economizer banks at the temperature of 350 °C and are sent to a selective catalytic reduction (SCR) unit for NO_x abatement. Flue gases are then cooled down to 120 °C in the air preheater, and particulates are removed with fabric filters. Air in-leakages have been assumed in the boiler and in the fabric filters, as fresh air infiltrations due to the negative gauge pressure kept in the boiler by a proper balance of the forced and induced draft fans. De-pulverized flue gas is sent to the wet flue gas desulfurizer (FGD) for SO₂ removal. A regenerative gas–gas heater (GGH) is used to heat up the saturated gas from the FGD system to secure the necessary lift of the flue gas and reduce the visibility of the plume at the stack.

The large-size steam turbine is simulated according to a stage-by-stage model [\[29\]](#), where each stage efficiency is calculated as a function of its non-dimensional parameters and of the moisture fraction when present in the low pressure stages. The high pressure turbine section features high reaction degree-high efficiency stages, whereas the low-pressure turbine section is based on two double-flow cylinders. In detail, the geometry of the last turbine stage is fixed, with a blade height of 104 cm, an exhaust area (per flow) of 10.4 m² and a peripheral velocity at mean diameter of 500 m/s. All these specifications are compatible with large state-of-the-art steam turbines [\[30\]](#). The resulting overall isentropic efficiencies of the turbine cylinders are 93.2%, 94.6% and 88.2% for high-, intermediate- and low-pressure sections respectively.

Heat from the condenser at 0.048 bar (32.1 °C) is rejected to the environment by means of cooling towers. Before feeding the boiler, the water from the condenser is preheated in four low-pressure (including the deaerator) and five high-pressure regenerative preheaters.

Details about the calculation assumptions for power plant modelling are reported in the Appendix as supplementary material.

3.2.2. Implementing the CO₂ capture system

The gas exiting the FGD system in [Fig. 3](#) is delivered by a blower through the adsorber (see [Fig. 1](#)) to overcome the pressure drop (~200 kPa). The regenerative gas–gas heater (GGH) in [Fig. 3](#) is removed as it would worsen the blower work. As shown in [Fig. 1](#), a conventional heat pump is adopted for the CSAR process: the low-temperature heat removed from the cooler and the adsorber is pumped to the desorber.

The heat pump system is based on ammonia vapor compression where the required pressure ratio, in the range from ~1.7 to ~2.3 depending on the CO₂ capture target (see [Section 4.2](#)), is moderate with a limited temperature increase throughout the compression. Thus, a properly sized single-stage centrifugal compressor is sufficient and intercooling is not necessary [\[31\]](#). Furthermore, a 3-stage vacuum pump for maintaining the desorber pressure at 0.1–0.2 bar (depending on the CO₂ capture target) as well as small evacuation pumps for the lock hoppers are included in the model.

The integration of the CSAR system with the PC-fired power plant should be simplified as much as possible to facilitate easy CO₂ capture retrofits. Nevertheless, injecting vacuum pressure steam in the upper regions of the desorber is an effective way to introduce an additional partial pressure swing. Hence, the last bleeding from the low-pressure turbine (at ~0.3 bar) is now directed to the CO₂ capture system as an efficient mode of heat integration without the need for modifications to the steam turbine assembly. As a consequence, the first water pre-heater does not receive heat from condensing steam but from the CO₂ capture station, considering the significant amount of low-temperature heat from the intercoolers of the 3-stage vacuum pump as well as of the 7-stage CO₂ compression system. The CO₂ stream at the outlet of each compressor stage is sufficiently warm (with temperature of ~90 °C) to replace the heat previously released by the steam from the last turbine bleeding. As a matter of fact, the heat from intercooling exceeds the duty at the first lower-temperature, water pre-heater, so auxiliaries for heat rejection are necessary.

Although large-scale coal-fired power plants generally have a steam bleed available at vacuum pressures, vacuum steam for the desorber can also be raised directly from the CO₂ compressors if proven necessary in specific cases. An assessment was done to show that such an arrangement loses only 0.27 %-points of efficiency relative to the default heat integration described above. Thus, even though the simulations presented in the subsequent results and discussion section assume the availability of vacuum steam from the power cycle, it is not a prerequisite for an efficient and non-invasive CO₂ capture retrofit using the CSAR technology.

In the case CO₂ capture is realized by the TSA technology, [Fig. 2](#) shows a relatively simpler system than [Fig. 1](#). Fans for driving flue gas and air through the heat exchangers present in the adsorber-to-desorber and desorber-to-adsorber paths, respectively, are included, and the outlet streams are recycled back at the inlet of the blower that is located upstream of the adsorber to overcome the pressure drop. Like the previous CSAR case, the regenerative gas–gas heater (GGH) in [Fig. 3](#) is removed.

Heat from sorbent carbonation in the adsorber is removed by cooling water, but steam is now necessary to supply the heat required for sorbent regeneration. The temperature of the steam is slightly lower than 100 °C, depending moderately on the CO₂ capture ratio (see [Section 4.2](#)), and is extracted along the expansion line. The warm condensate from the desorber is directed to the third low-pressure preheater, so the heat duties of the first two pre-heaters are lower compared to the reference plant without CO₂ capture. Also, the condenser duty reduces, though it is the same as the reference plant when considering CO₂ capture by the CSAR process. The same 7-stage CO₂ compression train from the CSAR case is implemented in the TSA configuration, but the heat recovery during intercooling is now rejected to the environment. Considering this heat rejection along with that from the adsorber, the overall duty of the TSA case is higher than the CSAR case.

Furthermore, no special considerations are made for the effect of steam extraction on the LP turbine efficiency because the effects are likely to be small and site-specific [\[32\]](#). Off-design operation of the turbine will reduce its efficiency, but the condenser will be able to achieve a lower pressure due to its reduced load, counteracting this effect to a certain extent.

Details about the calculation assumptions for CO₂ capture system modelling are reported in the Appendix as supplementary material.

3.3. Economic assessment

The standardized economic assessment (SEA) tool [33] was used to conduct the economic assessment, with the full SEA tool files available for download¹. The SEA tool allows for standardized bottom-up economic assessments that are comparable to previous works completed with the same methodology. In the present study, the capital cost assessments for the CSAR and TSA technologies were completed using cost correlations from Turton, Bailie [34] for basic process equipment like vessels, turbomachines, and heat exchangers. The total overnight cost of the coal-fired power plant was set to 2000 \$/kW (for the year 2020) based on IEA assumptions for Europe [35], whereas the total overnight cost of retrofitting the steam turbine and facilitating steam extraction was assumed to be 200 \$/kW (for the year 2009) following an IEAGHG assessment [32] on the topic.

Cost estimations of the reactors require assumptions regarding the reactor size, detailed in Table 4. Given the validated model assumption of chemical equilibrium in each CSTR, reactor size assumptions do not impact the model result, except for a small effect from the linear hydrostatic pressure profile representing the pressure drop. More importantly, the pressure drop assumed for the adsorber determines the flue gas blower capital cost and electricity demand.

The CSAR and TSA configurations use the same adsorber, which is sized for a 1 m/s superficial gas velocity and a gas residence time similar to that employed in the experimental demonstration of the SARC concept [17]. Assuming an average sorbent volume fraction of 0.25, the adsorber pressure drop is calculated to be 0.2 bar. The CSAR desorber is assumed to have half the cross-sectional area as the adsorber, designed to achieve similar fluidization behaviour to the adsorber according to fluidized bed regime correlations [36], whereas the TSA desorber has a 10x lower cross-sectional area than the adsorber to achieve a 2x higher superficial gas velocity, facilitating operation as a riser.

When the bare erected costs of all equipment are determined as described above, additional multipliers are used to yield the total overnight cost (Table 5). Subsequently, fixed and variable operating costs are added.

The determined total overnight cost and the fixed and variable operating costs are then used in a discounted cash flow analysis described in Eq. 1 and Eq. 2. The annual cash flow (ACF) is defined as the amount of revenue from electricity sales (S_{El}) [MWh/year at 100% plant availability] at a given average electricity sales price (P_{El}) [€/MWh] minus all the costs: variable operating and maintenance (C_{VOM}) [€/year at 100% plant availability], total overnight capital cost ($C_{Capital}$) [€/year], and variable operating and maintenance costs (C_{FOM}) [€/year]. $C_{Capital}$ is divided equally over the construction period of the plant, while revenues from electricity sales and variable operating costs are multiplied by the annual capacity factor of the plant (ϕ).

The ACF in each year (a) is then used to determine the net present value (NPV) of the plant in Eq. 2. Here, t starts upon plant construction

Table 4

Assumed dimensions and pressure drops for the reactors. Ten such reactor assemblies are required to treat the large flue gas stream from the coal-fired power plant.

Reactor	Adsorber	Desorber	
		CSAR	TSA
Diameter (m)	8.4	6.1	2.7
Height (m)	8.0	8.0	12.0
Pressure drop (bar)	0.2	0.2	0.1

Table 5

Economic evaluation assumptions [28,37–39].

Capital estimation methodology		
Bare Erected Cost (BEC)		SEA Tool Estimate
Engineering Procurement and Construction (EPC)		10% of BEC
Process Contingency (PS)		10%* or 30%** of BEC
Project Contingency (PT)		20% (BEC + EPC + PS)
Owners Costs (OC)		15% (BEC + EPC + PS + PT)
Total Overnight Costs (TOC)		BEC + EPC + PS + PT + OC
Operating & maintenance costs		
<i>Fixed</i>		
Maintenance	2.5	%TOC
Insurance	1	%TOC
<i>Variable</i>		
Coal	7	€/GJ
Sorbent	10	€/kg
CO ₂ transport & storage	10	€/ton
CO ₂ tax	100	€/ton
Process water	6	€/m ³
Cooling water make-up	0.35	€/m ³
Cash flow analysis assumptions		
1st year capacity factor	65	%
Remaining years	85	%
Discount Rate	8	%
Construction period	3	years
Plant Lifetime	25	years

* Turbomachines deployed in the CO₂ capture plants.

** Reactor vessels and internal heat exchange surfaces in the CO₂ capture plants.

and ends when after n years which is the sum of the construction and operating periods of the plant. Each consecutive year's ACF is discounted to a larger extent to represent the time value of money using the assumed discount rate (i).

$$ACF_t = \phi \hat{A} \cdot (P_{El} \hat{A} \cdot S_{El} - C_{VOM}) - C_{Capital} - C_{FOM} \quad (1)$$

$$NPV = \sum_{a=0}^n \frac{ACF_a}{(1+i)^a} \quad (2)$$

In the present study, the discounted cash flow analysis is used to yield three economic performance metrics. First, the levelized cost of electricity (LCOE) is determined as the electricity price (P_{El}) required to set the net present value of the plant to zero. Second, the net present value at an assumed electricity price is determined in certain cases. Finally, the CO₂ avoidance cost (CAC) [€/ton] is determined according to Eq. 3 using the LCOE [€/MWh] and specific emissions (E) [ton/MWh] of the plants with (CCS) and without (ref) CO₂ capture.

$$CAC = \frac{LCOE_{CCS} - LCOE_{ref}}{E_{ref} - E_{CCS}} \quad (3)$$

One important assumption to highlight from Table 5 is that the plant economic lifetime is assumed to be 25 years both for new plants and retrofits. The real lifetime of coal power plants, especially new builds, can be much longer, but investment decisions are typically made on shorter timeframes. Furthermore, extending the lifetime of the plant with the default discount rate of 8% has a minimal effect on the levelized costs because operating years beyond the 25-year economic lifetime is discounted so strongly. For example, cash flows from the 26th operating year are weighed at only 11% relative to cash flows from the first construction year with further declines in subsequent years.

4. Results and discussion

Results will be presented and discussed in four sections: 1) a basic techno-economic comparison of CSAR and TSA, 2) the effect of varying the CO₂ capture ratio, 3) the effect of lower capacity factors, and 4) a sensitivity analysis to other uncertain variables.

¹ <https://bit.ly/3wvJM6X>.

4.1. Basic comparison

The analysis revealed very similar techno-economic performance between the CSAR technology (driven by heat and vacuum pumps) and the TSA technology (driven by steam extracted from the power cycle). As illustrated in Fig. 4, both the power consumption and capital costs of the two plants are similar.

Regarding power consumption, the generation lost from the LP turbine in TSA is almost identical to the power consumption of the heat and vacuum pumps in CSAR. TSA also has a larger cooling water pump to facilitate heat removal from the adsorber. The total energy penalties are 8.0 and 8.2 %-points for CSAR and TSA, respectively, considerably lower than a values of 10.3 and 10.9 %-points calculated by Riboldi et al. [22] for an adsorption-based fixed bed VPSA process and an MEA benchmark, respectively. Relative to an MEA process, the CSAR and TSA processes benefit from the low regeneration enthalpy of the PEI sorbent employed. Relative to the two-stage VPSA process, the single-stage CO₂ separation in CSAR and TSA facilitated by the temperature swing brings significant efficiency benefits. However, it should be noted that advanced solvents such as piperazine amino-methyl-propanol can reduce the energy penalty of CO₂ capture from coal-fired power plants by as much as 2.8 %-points [9], achieving similar efficiencies to the sorbent-based CSAR and TSA processes. High-temperature adsorption via Ca-looping can achieve even better efficiencies (7.0 %-point energy penalty [40]) by utilizing the high-grade heat released during CO₂ capture for power production, but the retrofit operation is much more extensive due to the need for an air separation unit and power cycle in addition to the high-temperature (650–920 °C) adsorption reactors.

The capital cost assessment shows that the CSAR heat and vacuum pumps are cheaper than the steam cycle modifications required in the TSA setup. On the other hand, CSAR has a considerably larger desorber due to the vacuum conditions that require a larger cross-sectional area to prevent excessive particle elutriation, leading to higher reactor costs. Other reactor costs remain similar as the adsorber and cooler are identical and the lock hoppers in CSAR have a similar cost to the recuperative heat exchangers in TSA.

As may be anticipated from Fig. 4, Fig. 5 shows near identical economic performance between CSAR and TSA. At the assumed CO₂ price of 100 €/ton, both options are considerably cheaper than an unabated coal plant because CO₂ can be avoided for 46–55 €/ton. Fig. 5 also shows the difference between the extreme cases of 1) retrofitting a new coal-fired power plant that is not yet depreciated with post-combustion CO₂ capture and 2) retrofitting a coal plant that is already fully depreciated or has become a stranded asset. When retrofitting such a depreciated coal plant, the only capital cost in the assessment is that of the CO₂ capture facility as the capital cost of the power plant itself can be assumed to be

zero. The result is a 31 €/MWh reduction in LCOE relative to the case of a new power plant. The CO₂ avoidance cost also reduces by 8 €/ton because the higher levelized capital cost caused by the energy penalty of CO₂ capture is avoided when the power plant capital cost is set to zero. It is noted that the TSA process would have a significant advantage when building a greenfield plant with post-combustion CO₂ capture because there will be no dedicated turbine modification costs and the LP turbine and condenser can be reduced in size.

Fig. 5 also shows that the CO₂ capture plants have considerably higher fixed and variable operating and maintenance costs than the unabated plant. Increased fixed costs arise from a larger amount of capital to maintain and insure, whereas greater variable costs originate from the additional costs of CO₂ transport and storage and sorbent replacement. Coal costs also increase due to the lower efficiency of the CO₂ capture plants. Although CO₂ capture greatly reduces CO₂ costs, the CO₂ price of 100 €/ton significantly inflates the LCOE of the CO₂ capture plants at the 90% capture ratio assumed.

4.2. Effect of CO₂ capture ratio

As Fig. 5 showed, high CO₂ prices impose a significant cost on coal-fired power plants even if 90% of the CO₂ is captured. Hence, it is of interest to investigate retrofits designed for higher CO₂ capture ratios. In both plants, the CO₂ capture ratio is manipulated by adjusting the desorber temperature, with higher temperatures facilitating a higher degree of desorption which creates a lower equilibrium partial pressure at the top of the adsorber, leading to higher CO₂ capture ratios. A higher desorber temperature will increase the energy penalty of CO₂ capture for both concepts. In CSAR, the heat pump becomes less efficient when a higher temperature swing is employed, while steam extraction at a higher temperature leads to a larger loss in LP steam turbine power output in TSA.

Fig. 6 shows that the heat pump-related efficiency losses in CSAR are substantially larger than the steam turbine output losses in TSA when the CO₂ capture ratio is increased. Hence, even though the energy penalty of the two plants is essentially identical at 90% capture, CSAR imposes a 1.4 %-point greater energy penalty when the CO₂ capture ratio is increased to 98%.

The effect of this trade-off in more energy penalty for greater CO₂ capture is illustrated in Fig. 7. Clearly, when the CO₂ price is set to 100 €/ton, increasing the CO₂ capture ratio beyond 90% is beneficial, especially for the TSA technology. However, even CSAR benefits from higher CO₂ capture ratios, although the rapidly rising energy penalty cancels out falling CO₂ costs when increasing the capture ratio from 95% to 98%. At 98% capture, the LCOE of TSA is 3% below that of CSAR.

As an additional benefit, CSAR may offer some flexibility regarding

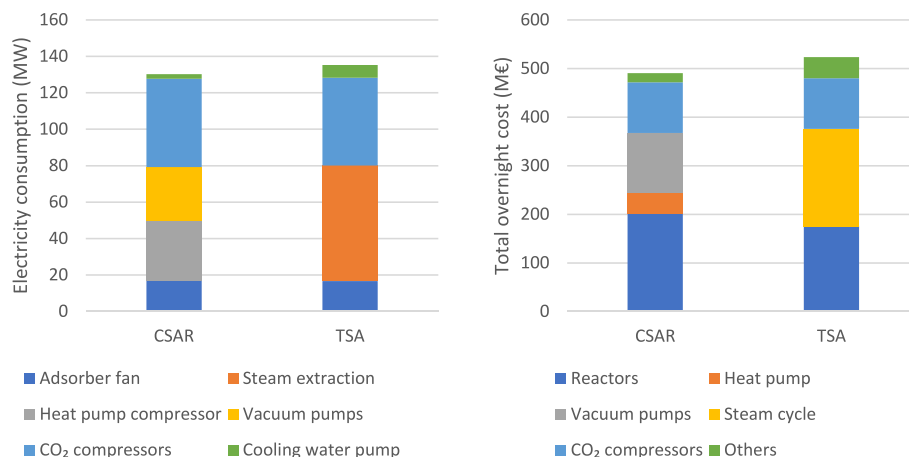


Fig. 4. A breakdown of the power consumption (left) and capital costs (right) for capturing CO₂ using CSAR and TSA technologies.

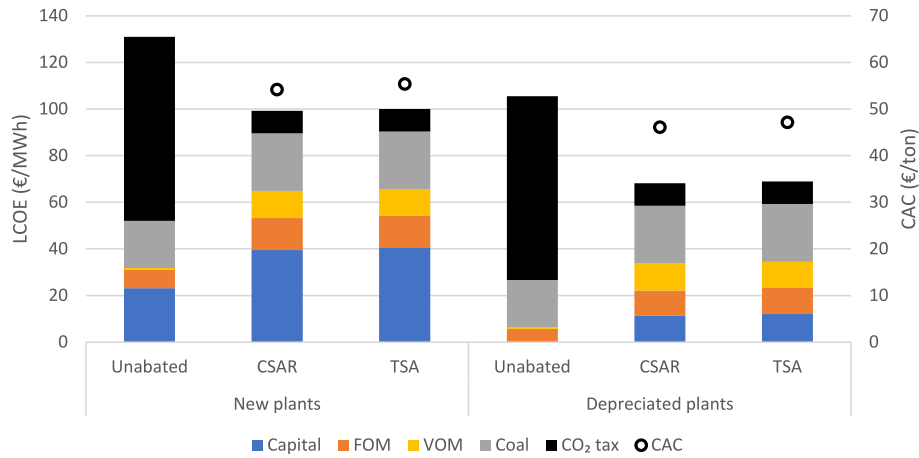


Fig. 5. Levelized costs of electricity (LCOE) and CO₂ avoidance costs (CAC) for CSAR and TSA technologies retrofitted to a new (undepreciated) and fully depreciated coal power plants, assuming a 100 €/ton CO₂ price and 90% CO₂ capture. The depreciated coal plant is assumed to have zero value. FOM = fixed operating and maintenance costs and VOM = variable operating and maintenance costs.



Fig. 6. The effect of CO₂ capture ratio on the energy penalty of CSAR and TSA technologies fitted to a coal-fired power plant.

the trade-off between CO₂ capture ratio and electricity consumption by operating the heat pump compressor and expansion valve with a mild degree of flexibility to adjust the compression ratio. Increasing the compression ratio of the ammonia compressor will cause a greater temperature swing in the heat pump and thus exchange more CO₂ capture for higher electricity consumption. Such flexibility could bring significant economic benefits in a market of volatile CO₂ and electricity prices. In comparison, there is little scope for changing the temperature of the extracted steam to provide flexibility regarding the CO₂ capture ratio in the TSA configuration.

More importantly, the economic performance of CSAR remains on par with that of TSA across the range of CO₂ capture ratios investigated. Since CSAR should be substantially simpler to install as a retrofit than TSA, it would be the preferred solution if overall economic performance is similar.

4.3. The effect of reduced capacity factor operation

Despite their high CO₂ emissions, coal-fired power plants will be difficult to remove from the power system by rising CO₂ taxes in natural gas-importing regions. Growth in wind and solar power will reduce the capacity factors of existing coal-fired plants, but most of the dispatchable capacity will still be required to ensure reliable power production during extended periods of low wind and sun. During such periods, the market price will rise strongly to incentivise coal power plants to produce power despite high CO₂ taxes. Such high prices will be compensated to a certain degree by low (or even negative) prices when wind and solar power output is high, meaning that the long-term average electricity price experienced by consumers remains reasonable.

In the absence of explicit coal phase-out policies that override market forces, coal-fired power plants will only become stranded assets when high CO₂ prices make it profitable to shut down the plant and build new dispatchable generators for meeting demand during expended periods of low wind and solar output in its place. Natural gas or hydrogen-fired power plants are the most likely alternatives, but Fig. 8 shows that continued operation of a fully depreciated coal plant will remain preferable to new gas-fired plants even at CO₂ prices of 100 €/ton when the capacity factor is only 20%. Furthermore, storage of natural gas or hydrogen for enabling such low capacity factor operation will add substantial additional costs to new gas-fired plants (ignored in Fig. 8). Hence, it is likely that CO₂ prices will need to rise well above 100 €/ton before existing coal-fired power plants are completely driven out of the market in natural gas importing regions.

Fig. 9 offers an illustration of this effect by comparing the levelized costs of zero-value coal plants operated at different capacity factors to the average electricity prices that may be expected under such operating conditions. Illustrative electricity prices are taken for North Germany based on a previous study of a mid-century near-zero-emission energy system coupled between Germany and Norway [41]. As illustrated, if a dispatchable power plant operates only in the 20% most expensive hours of the year, it could access electricity prices averaging 159 €/MWh. However, when operating in all but the 20% cheapest hours of the year, its average electricity price drops down to 87 €/MWh. It is noted that these modelled electricity prices may be considered to be conservatively low because a 5% discount rate was used in the system-scale model to reflect the low financing costs created by supporting policies for wind and solar power (as opposed to the 8% discount rate assumed in Table 5).

As anticipated from the discussion above, the unabated depreciated coal plant remains profitable (LCOE below the electricity price) when it can operate at low capacity factors during times of high electricity

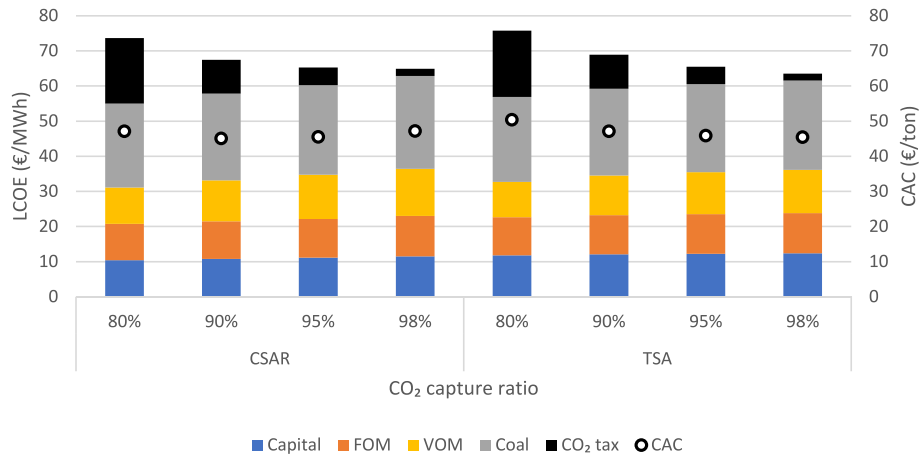


Fig. 7. The economic performance of CSAR and TSA plants retrofitted to stranded asset (zero value) coal power plants. LCOE = levelized cost of electricity, CAC = CO₂ avoidance cost, FOM = fixed operating and maintenance cost, VOM = variable operating and maintenance cost.

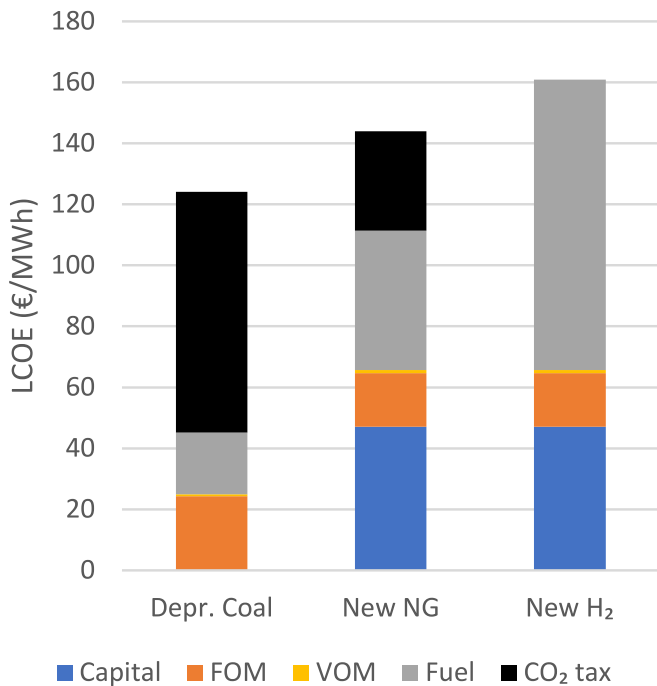


Fig. 8. A comparison of the economic attractiveness of continuing to run a fully depreciated coal-fired power plant at a low capacity factor of 20% relative to building new combined cycle power plants burning less carbon-intensive fuels. The capital cost of the 63% efficient combined cycle natural gas (NG) and hydrogen (H₂) plants is assumed to be 800 €/kW, whereas imported natural gas is assumed to cost 8 €/GJ and zero-carbon hydrogen 2 €/kg (16.7 €/GJ).

prices. The assumption that the coal plant is already fully depreciated is crucial to this finding because it avoids large increases in the levelized cost of capital when capital investments must be recovered over a smaller number of operating hours implied by low capacity factors. A new unabated coal plant would be uneconomical under all capacity factors as it would be unable to generate enough operating profit to recover its substantial upfront investment under the assumed 8% discount rate.

Fig. 9 also shows that depreciated coal-fired power plants retrofitted with CSAR capturing 95% of the produced CO₂ remain profitable at all four investigated capacity factors, although the profitability gap shrinks when the capacity factor drops as low as 20%. At such low capacity factors, the levelized capital costs of the CO₂ capture facility become

large due to the small amount of electricity over which these fixed costs must be levelized. The same is true for the fixed operating and maintenance costs, which include maintenance of both the CO₂ capture facility and the coal-fired power plant.

In practice, there will be additional costs associated with more part-load operation and frequent plant shutdowns and restarts. However, it may also be possible to reduce fixed operating and maintenance costs when the plant is operated less frequently than usual, especially when the frequency of cold starts can be minimized. For example, in a system with a high reliance on wind power and/or a highly seasonal solar generation profile, the plant may be shut down for several weeks/months of moderate to high renewable energy output, followed by a few weeks/months of operation during an extended period of low renewable energy output. Taking the 20% capacity factor case as an example, a halving of the fixed operating and maintenance costs relative to the 80% capacity factor case (which still entails a doubling of maintenance costs per unit electricity produced) can cancel out costs related to flexible operation equivalent to a 12% reduction in the plant efficiency. Due to these counterbalancing factors, the results in Fig. 9 should be reasonable.

Fig. 10 presents the results from a different perspective: net present value. The net present value is the cumulative discounted cash flow at the end of the economic lifetime of the plant, and it should be positive for the project to be considered economically attractive. It is immediately evident that new coal-fired power plants, either with or without CO₂ capture are not financially viable. However, fully depreciated power plants will remain economically attractive under most operating conditions with the electricity market prices indicated in Fig. 9.

Furthermore, retrofitting with CSAR allows the depreciated coal plant to continue operating profitably at high capacity factors, whereas unabated plants must operate at low capacity factors to maximize profitability. When capacity factors fall to very low levels, the absence of capital costs in the unabated plant gives it a lower levelized cost than the more capital-intensive retrofit, despite the high operating costs from CO₂ taxation. However, the unabated plant will be highly sensitive to fluctuations in the CO₂ price with prices above 170 €/ton rendering it unprofitable even at a 20% capacity factor. This concurs with the simple assessment presented in Fig. 8 where a 150 €/ton CO₂ price inflates the LCOE of the depreciated coal plant to that of new natural gas or hydrogen plants (excluding additional gaseous fuel storage costs). Under such conditions, the coal-fired power plant would become a true stranded asset that must be retired before the end of its technical lifetime and replaced by alternatives.

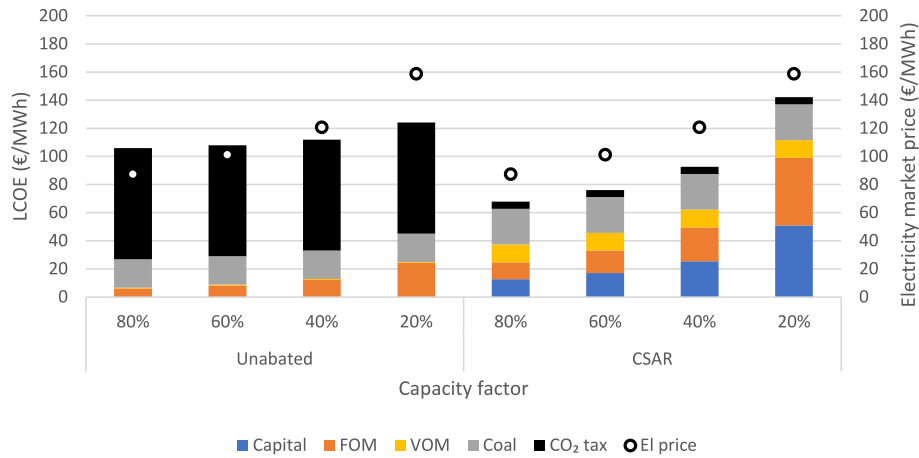


Fig. 9. The economic performance of fully depreciated coal power plants without (unabated) and with CSAR retrofits under a range of capacity factor assumptions. The circles illustrate the higher average electricity prices that can be accessed when operating only during the most expensive hours of the year in Germany by 2050 [41]. LCOE = levelized cost of electricity, CAC = CO₂ avoidance cost, FOM = fixed operating and maintenance cost, VOM = variable operating and maintenance cost.

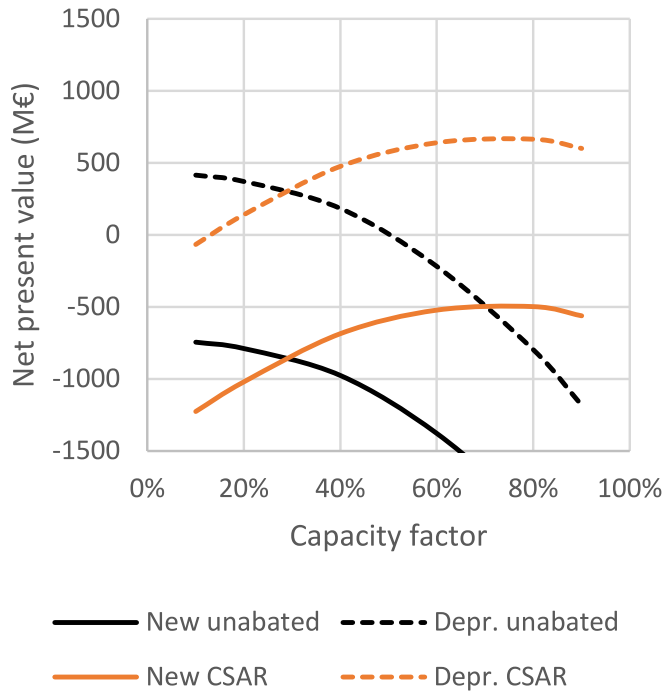


Fig. 10. The net present values achieved by new and depreciated coal plants with and without a CSAR retrofit at different capacity factors when the plant has access to the electricity market prices illustrated in Fig. 9.

4.4. Sensitivity analysis

Aside from the CO₂ capture ratio and capacity factor studied in previous sections, Fig. 11 shows the sensitivity to four additional uncertain variables in the current assessment. The analysis was completed for a fully depreciated coal-fired power plant either operated with or without a CSAR retrofit. Mid-load operation at a 50% capacity factor is assumed in anticipation of growing shares of variable renewables and the CSAR retrofit is assumed to capture 95% of the produced CO₂. The TSA alternative is not shown as it returns almost identical behaviour to CSAR.

The sensitivity to coal prices increases when the CO₂ capture retrofit is completed due to the energy penalty involved in capturing CO₂, but the generally low price of coal limits the impact of this parameter on the LCOE. On the other hand, the highly uncertain CO₂ price poses a major

risk to the unabated plant, causing the LCOE to increase by a factor of 6 when CO₂ prices rise from 0 to 200 €/ton. A CSAR retrofit reduces this sensitivity by a factor of 16. However, CO₂ capture introduces another sensitivity: the cost to transport and store the captured CO₂. For a limited number of plants, CO₂ can even be handled at a profit for applications such as enhanced oil recovery or a wide range of other emerging CO₂ utilization opportunities. Still, the majority of CO₂ captured from coal-fired power plants will need to be sequestered at a cost in suitable underground formations. The cost related to this operation will depend mainly on the proximity of the plant to a suitable storage site. Lastly, the contingency added to the CSAR capital cost does not have a major impact on the LCOE. Increasing the contingency factor from 0 to 2 implies a 32% increase in the CSAR plant capital cost, increasing the LCOE by only 9%.

5. Summary and conclusions

The world has a large fleet of relatively young coal-fired power plants, particularly in Asia. By themselves, these plants will consume the entire CO₂ budget for 1.5 °C of global warming if they run to the end of their technical lifetimes. Retrofits with CO₂ capture represent an attractive solution to this challenge, and the continuous swing adsorption reactor (CSAR) concept can facilitate such retrofits in a practical and cost-effective manner.

CSAR uses a synergistic combination of heat and vacuum pumps to drive the CO₂ capture process. Since these units require only electric energy to run, CSAR does not need steam extraction from the power cycle of the coal plant, greatly simplifying the retrofit process. Techno-economic assessment results from this study illustrated that CSAR can capture CO₂ at a similar efficiency and cost as the conventional method of extracting steam from the power cycle to regenerate the sorbent. When the economic performance is similar, CSAR will be the preferred solution due to its ease of retrofitting and potential for flexibly varying the CO₂ capture ratio in response to fluctuating electricity and CO₂ prices.

Economic assessments completed for coal-fired power plants operating under different capacity factors revealed that the construction of new plants in an environment of high CO₂ prices is not economically viable, whether equipped with CO₂ capture or not. However, continued operation of fully depreciated coal plants will remain viable under most market conditions. As the share of variable renewable energy grows, dispatchable generators will still be required in most markets to ensure security of supply during extended periods of low wind and solar output. A fully depreciated power plant holds a large advantage under these low capacity factor conditions compared to new plants that still need to

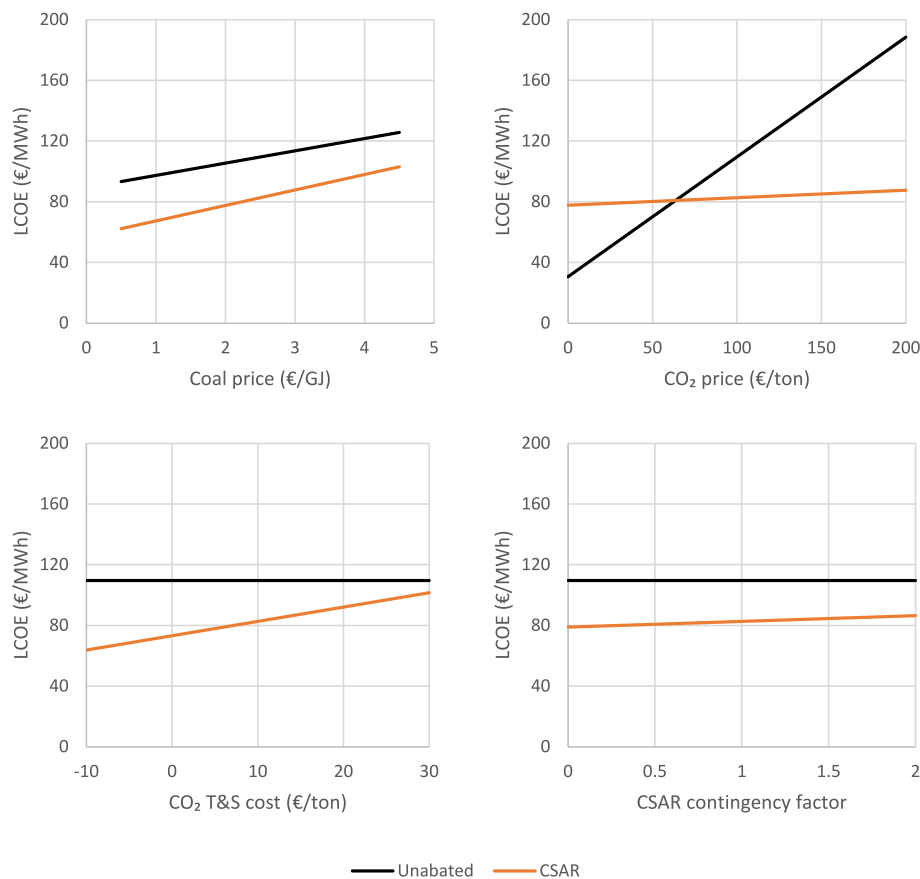


Fig. 11. Sensitivity of the levelized cost of electricity of fully depreciated coal-fired power plants operated at a 50% capacity factor without (unabated) and with 95% CO₂ capturing using CSAR. The contingency factor is a factor by which the baseline process contingencies assumed for CSAR (30% for the reactors and 10% for the turbomachines) are multiplied.

recover their upfront investment. In such an environment, results showed that very high CO₂ prices in excess of 150 €/ton would be required to incentivize early retirement of an already depreciated coal plant and replace it with a new natural gas or hydrogen-fired power plant.

Alternatively, the depreciated coal plant can be retrofitted with a CO₂ capture facility such as CSAR at much lower costs (below €50 per ton of avoided CO₂). In this event, profitable baseload operation can continue in an environment of high CO₂ prices. As the upfront investment of the CO₂ capture facility must still be recovered in this case, the economic attractiveness reduces when the plant operates at low capacity factors. In the present assessment assuming a CO₂ price of 100 €/ton, a CO₂ capture retrofit became economically unattractive when the plant capacity factor falls below 30%.

This dynamic suggests a partial retrofit strategy for natural gas importing regions with a large fleet of relatively young coal-fired power plants. Plants conveniently located close to CO₂ storage reservoirs or CO₂ utilization opportunities should be retrofitted for CO₂ capture and continue serving as baseload generators. On the other hand, plants located far away from such facilities should gradually reduce their annual operating hours to facilitate increasing shares of wind and solar power. In addition to a large, rapid, and economical reduction in CO₂ emissions, this strategy will facilitate a gradual and non-disruptive ramp-down of the large coal supply industries operating in countries reliant on coal-fired power production.

CSAR can accelerate this important transition by removing technical

barriers to retrofitting a large fleet of different types of coal-fired power plants with CCS. In the more conventional TSA pathway, steam extraction from the low-pressure steam turbines of various power cycle designs will impose substantial practical challenges, slowing down the transition and potentially imposing unforeseen costs and extended plant downtime during the retrofit project. For these reasons, practical and cost-effective CO₂ capture retrofit technologies such as CSAR can greatly benefit the global decarbonization effort.

Declaration of Competing Interest

The authors declare that they have no known competing financial interests or personal relationships that could have appeared to influence the work reported in this paper.

Data availability

Data will be made available on request.

Acknowledgement

This study was partly funded under the Climit-Demo project “Verification and demonstration of an advanced adsorption reactor for cost effective CO₂ capture” with the grant number 621172. The internal financial support from SINTEF for preparing the draft is also acknowledged.

Appendix

This section reports the main assumptions for the calculation of the mass and energy balance of the PC-USC power plant even considering both the CSAR and TSA processes as well as CO₂ compression.

See Table A1-A4.

Table A1

Main assumptions for the calculation of the steam power plant without CO₂ capture.

<i>Pulverized coal boiler</i>	
Coal composition, %wt.: 66.52% C; 3.78% H; 1.56% N; 5.46% O; 0.52% S; 14.15% Ash; 8.01% H ₂ O	
Coal lower heating value, MJ/kg	25.17
Coal higher heating value, MJ/kg	26.23
Heat input, MW _{LHV}	1657.1
Primary/secondary air, %	25/75
Pressure losses in air preheater (each side), kPa	1
Pressure losses in mills and burners (I air), kPa	6.3
Pressure losses in windbox and burners (II air), kPa	3.3
Pressure losses in convective pass, SCR and FF, kPa	3.5
Pressure losses in FGD, kPa	2
Pressure losses in FGD gas–gas heater (each side), kPa	1
Furnace pressure, bar	1.01
Losses for radiation and unconverted C, % of coal lower heating value	0.35
Heat loss in heat exchangers, % of heat transferred	0.5
Oxygen concentration in flue gas at boiler exit, %vol.	2.9
Air in-leakages in the boiler, %wt. of flue gas	1
Air in-leakages at FF, %wt. of flue gas	5
Gas temperature at economizer outlet, °C	350
Hot gas temperature at air preheater outlet, °C	120
<i>Boiler auxiliaries</i>	
Fan isentropic efficiency, %	80
Fan electric-mechanical efficiency, %	94
Coal handling and milling, kJ _e /kg _{coal}	50
Ash handling systems, kJ _e /kg _{ash}	200
Flue gas desulfurization, kJ _e /kg _{SO2}	5340
Miscellaneous BOP, % of input LHV	0.15
<i>Steam cycle</i>	
Boiler feedwater pressure, bar	320
Live steam temperature SH/RH, °C	600/620
Live steam pressure SH/RH, bar	270/60
SH/RH piping thermal losses, °C	2
SH/RH steam pressure losses at turbine inlet valve, %	2
RH steam pressure loss, bar	4
Condensing pressure, kPa	4.8
Number of LP/HP preheaters	4/5
Pressure of steam bled for LP feedwater preheaters, bar	93.8/64.0/39.2/23.7
Pressure of steam bled for HP feedwater preheaters, bar	14.6/6.7/3.5/1.26/0.32
Pinch-point ΔT in preheaters, °C	3
Steam pressure losses in deaerator / HP preheaters, %	7/3
Feedwater pump hydraulic efficiency, %	85
Feedwater pump mechanical/electric efficiency, %	98.5/95
Auxiliaries for heat rejection to environment, kJ _e /MJ _{th}	8
<i>Steam turbine</i>	
Rotational speed, rpm	3000
Number of HP/IP/LP parallel flows	1/1/4
Crossover pressure, bar	5.2
Isentropic stage efficiency, %	calculated [29]
Last stage turbine blade height, m	1.04
Last stage peripheral velocity at mean diameter, m/s	500
Last stage exhaust area (per flow), m ²	10.4
Exhaust steam velocity, m/s	220
Steam turbine mechanical efficiency, %	99.6
Electric generator efficiency, %	98.5

Table A2

Main assumptions for the calculation of the CSAR process.

Pressure loss through the adsorber, bar	0.2
Main blower isentropic efficiency, %	80
Main blower electric-mechanical efficiency, %	94
Desorber pressure*, bar	0.15
Overall heat supplied by the heat pump*, MW	327.5
Overall heat removed by the heat pump *, MW	297.7
Overall heat removed by cooling water*, MW	43.3
Ammonia evaporation temperature*, °C	51.4
Ammonia condensation temperature*, °C	76.2

(continued on next page)

Table A2 (continued)

Pressure loss through the adsorber, bar	0.2
Ammonia compressor isentropic efficiency, %	85
Ammonia compressor electric-mechanical efficiency, %	94
Evacuation pressure at toppler lock-hopper*, bar	0.15
Evacuation pressure at bottomer lock-hopper*, bar	0.7
Vacuum pump stages*	3
Vacuum pump isentropic stage efficiency, %	85
Vacuum pump electric-mechanical efficiency, %	94
Fluid temperature after each intercooling stage, °C	35
Desorber recycle fan isentropic efficiency, %	80
Desorber recycle fan electric-mechanical efficiency, %	94

* in the case of 90% CO₂ capture ratio.**Table A3**

Main assumptions for the calculation of the TSA process.

Pressure loss through the adsorber, bar	0.2
Main blower isentropic efficiency, %	80
Main blower electric-mechanical efficiency, %	94
Desorber pressure, bar	1
Overall heat supplied by steam*, MW	514.3
Steam condensing temperature*, °C	92.7
Overall heat removed by cooling water*, MW	530
Overall heat recovery at the recuperator*, MW	128
Cooler/heater recycle fan isentropic efficiency, %	80
Cooler/heater recycle fan electric-mechanical efficiency, %	94

* in the case of 90% CO₂ capture ratio.**Table A4**Main assumptions for the calculation of the CO₂ compression station.

CO ₂ compressor stages	7
CO ₂ compressor isentropic stage efficiency, %	85
CO ₂ compressor electric-mechanical efficiency, %	95
CO ₂ temperature after each intercooling stage, °C	35
CO ₂ aftercooling temperature, °C	25
CO ₂ pressure loss at intercoolers, %	1
CO ₂ pump isentropic efficiency, %	75
CO ₂ pump electric-mechanical efficiency, %	92
CO ₂ pumping pressure start/delivery, bar	80/110

References

- [1] IPCC, Climate Change 2021: The Physical Science Basis, in the Sixth Assessment Report. 2021, Intergovernmental Panel on Climate Change.
- [2] IPCC, Climate Change 2022: Mitigation of Climate Change, in the Sixth Assessment Report. 2022, Intergovernmental Panel on Climate Change.
- [3] Anon. Plant Tracker: Summary Statistics. 2022; Available from: <https://globalenergymonitor.org/projects/global-coal-plant-tracker/dashboard/>.
- [4] Gapminder. Global income mountains. 2022; Available from: <https://www.gapminder.org/fw/income-mountains/>.
- [5] IEA, Special report on carbon capture utilization and storage: CCUS in clean energy transitions, in Energy Technology Perspectives. 2020.
- [6] S. Giannaris, et al., Implementing a second generation CCS facility on a coal fired power station – results of a feasibility study to retrofit SaskPower's Shand power station with CCS, Greenhouse Gases Sci. Technol. 10 (3) (2020) 506–518.
- [7] E.S. Rubin, J.E. Davison, H.J. Herzog, The cost of CO₂ capture and storage, Int. J. Greenhouse Gas Control 40 (2015) 378–400.
- [8] IEA, World Energy Outlook. 2022, International Energy Agency.
- [9] P.H.M. Feron, et al., An update of the benchmark post-combustion CO₂-capture technology, Fuel 273 (2020), 117776.
- [10] R.-S. Liu, et al., Advances in post-combustion CO₂ Capture by physical adsorption: from materials innovation to separation practice, ChemSusChem 14 (6) (2021) 1428–1471.
- [11] D. Bhattacharyya, D.C. Miller, Post-combustion CO₂ capture technologies — a review of processes for solvent-based and sorbent-based CO₂ capture, Curr. Opin. Chem. Eng. 17 (2017) 78–92.
- [12] J.-X. Guo, C. Huang, Feasible roadmap for CCS retrofit of coal-based power plants to reduce Chinese carbon emissions by 2050, Appl. Energy 259 (2020), 114112.
- [13] J.-L. Fan, et al., Carbon capture and storage (CCS) retrofit potential of coal-fired power plants in China: The technology lock-in and cost optimization perspective, Appl. Energy 229 (2018) 326–334.
- [14] N. MacDowell, et al., An overview of CO₂ capture technologies, Energ. Environ. Sci. 3 (11) (2010) 1645–1669.
- [15] H.C. Mantripragada, H. Zhai, E.S. Rubin, Boundary Dam or Petra Nova – Which is a better model for CCS energy supply? Int. J. Greenhouse Gas Control 82 (2019) 59–68.
- [16] M. Lucquiaud, J. Gibbins, Steam cycle options for the retrofit of coal and gas power plants with postcombustion capture, Energy Procedia 4 (2011) 1812–1819.
- [17] C. Dhoke, et al., Demonstration of the Novel Swing Adsorption Reactor Cluster Concept in a Multistage Fluidized Bed with Heat-Transfer Surfaces for Postcombustion CO₂ Capture, Ind. Eng. Chem. Res. 59 (51) (2020) 22281–22291.
- [18] C. Dhoke, et al., The swing adsorption reactor cluster (SARC) for post combustion CO₂ capture: Experimental proof-of-principle, Chem. Eng. J. (2018).
- [19] S. Cloete, et al., Economic assessment of the swing adsorption reactor cluster for CO₂ capture from cement production, J. Clean. Prod. 275 (2020), 123024.
- [20] S. Cloete, et al., The swing adsorption reactor cluster for post-combustion CO₂ capture from cement plants, J. Clean. Prod. 223 (2019) 692–703.
- [21] Z. Liu, et al., Onsite CO₂ capture from flue gas by an adsorption process in a coal-fired power plant, Ind. Eng. Chem. Res. 51 (21) (2012) 7355–7363.
- [22] L. Riboldi, O. Bolland, Evaluating pressure swing adsorption as a CO₂ separation technique in coal-fired power plants, Int. J. Greenhouse Gas Control 39 (2015) 1–16.
- [23] W. Si, et al., Deactivation kinetics of polyethylenimine-based adsorbents used for the capture of low concentration CO₂, ACS Omega 4 (6) (2019) 11237–11244.
- [24] W. Choi, et al., Epoxide-functionalization of polyethylenimine for synthesis of stable carbon dioxide adsorbent in temperature swing adsorption, Nat. Commun. 7 (1) (2016) 12640.
- [25] C. Dhoke, et al., Study of the cost reductions achievable from the novel SARC CO₂ capture concept using a validated reactor model, Ind. Eng. Chem. Res. 60 (33) (2021) 12390–12402.
- [26] C. Dhoke, et al., Sorbents screening for post-combustion CO₂ capture via combined temperature and pressure swing adsorption, Chem. Eng. J. 380 (2020), 122201.
- [27] H.M. Kvamsdal, et al., Energetic evaluation of a power plant integrated with a piperazine-based CO₂ capture process, Int. J. Greenhouse Gas Control 28 (2014) 343–355.
- [28] F. Franco, et al., European Best Practice Guidelines for CO₂ Capture Technologies, in: CESAR project: European Seventh Framework Programme. 2011.

- [29] G. Lozza, Bottoming steam cycles for combined gas–steam power plants: a theoretical estimation of steam turbine performance and cycle analysis. In: Proceedings of the 1990 ASME Cogen-Turbo. 1990. New Orleans (LO), USA.
- [30] A.S. Leyzerovich, *Steam Turbines for Modern Fossil-Fuel Power Plants*, The Fairmont Press, 2008.
- [31] A. Zaabout, et al., Thermodynamic assessment of the swing adsorption reactor cluster (SARC) concept for post-combustion CO₂ capture, *Int. J. Greenhouse Gas Control* 60 (Supplement C) (2017) 74–92.
- [32] IEAGHG, Retrofitting CO₂ capture to existing power plants 2011, International Energy Agency.
- [33] C. Arnaiz del Pozo, S. Cloete, Á. Jiménez Álvaro. Standard Economic Assessment (SEA) Tool. Available from: <https://bit.ly/3IXPWC8>, 2021.
- [34] R. Turton, et al., *Analysis, synthesis and design of chemical processes*: Appendix A. 2008: Pearson Education.
- [35] IEA, *World Energy Outlook*. 2021, International Energy Agency.
- [36] H.T. Bi, J.R. Grace, *Flow regime diagrams for gas-solid fluidization and upward transport*, *Int. J. Multiph. Flow* 21 (6) (1995) 1229–1236.
- [37] S2BIOM, S2BIOM integrated tool set. 2022, <https://s2biom.wenr.wur.nl/web/guest/home>.
- [38] E. Rubin, et al., Toward a common method of cost estimation for CO₂ capture and storage at fossil fuel power plants. 2013, Global CCS institute.
- [39] J. Adanez, et al., Progress in Chemical-Looping Combustion and Reforming technologies, *Prog. Energy Combust. Sci.* 38 (2) (2012) 215–282.
- [40] M. Astolfi, E. De Lena, M.C. Romano, Improved flexibility and economics of Calcium Looping power plants by thermochemical energy storage, *Int. J. Greenhouse Gas Control* 83 (2019) 140–155.
- [41] S. Cloete, et al., Blue hydrogen and industrial base products: The future of fossil fuel exporters in a net-zero world, *J. Clean. Prod.* 363 (2022), 132347.